JOURNAL OF MATERIALS SCIENCE 26 (1991) 4433–4438

Mechanism of crystallization of multi-component metallic coatings using the impulse plasma method

K. ZDUNEK
Institute of Materials Science, Warsaw University of Technology, 85 Narbutta, 02-524 Warsaw, Poland

The impulse plasma method was used to obtain complex metallic coatings. Taking into account the way of the central electrode of an impulse plasma accelerator is worn, and the features of the coatings, a mechanism for crystallization of metallic coatings from impulse plasma is proposed.

1. Introduction

The method of crystallizing a coating from pulsed plasma was developed at the Institute of Materials Science, Warsaw University of Technology, in the late 1970s [1]. The impulse plasma is generated in a coaxial accelerator working in quasistationary mode [2] and accelerated by its own electromagnetic force [3] to a velocity of the order of 10^4 m s^{-1} [4]. Owing to the pulsed character of the process, whose most essential feature is that the crystallization centre remains at a high thermodynamic temperature (of the order of 2×10^3 K [5]) for an extremely short time (about 10^{-4} s [2]), the solid phase condensed in the presence of charged particles is ultra-fine crystalline [6, 7].

Diamond coatings, TiN coatings and metallic coatings have been obtained using the impulse plasma method [8–10]. The present work aimed to describe the formation mechanism of complex metallic coatings crystallizing from the impulse plasma.

2. Experimental procedure

The apparatus used for the investigations and the principle of its operation have been described earlier (e.g. [2]). Fig. 1 shows a schematic representation of it.

A 12 mm diameter heat-treated Co–25Cr–9Al rod was used as the central electrode of the coaxial generator of pulsed plasma. The plasma processes (i.e. the generation of the pulsed plasma, and the condensation of the coating) were carried out in an H_2 atmosphere under a pressure of 20 Pa. The energy source for the process was a battery of condensers (with capacitances ranging from 175–225 μF) charged to 6–7 kV. The substrates made of 1 mm thick nickel sheet were positioned centrally (along the axis of the plasma generator) or radially (45 mm away from the generator axis) at a distance of 160–270 mm from the generator outlet. No external source was used to heat the substrates before, during or after the plasma process. Each process consisted of about 550 pulses repeated at a frequency of 0.1 Hz.

The materials were examined using metallographic methods, Vickers and Rockwell hardness measurements, X-ray diffraction (XRD), and also by means of an X-ray microprobe.

3. Results

3.1. The central electrode material

Table I gives the phase compositions of the material of the central electrode of the plasma generator. It can be seen that this material is built up of two phases, the β-AlCo phase in the matrix of the Co(Cr, Al) solid solution.

Fig. 2 shows how the central electrode looks before and after the process (pulse number ~ 15 000). The electrode undergoes wear during the process: the diameter of the electrode in its cylindrical part remained unchanged, but operation of the electrode resulted in its shortening (approximately 1 mm per 1000 impulses). As early as after several hundred pulses, the flat surface of its free end becomes "bowl"-shaped 5–6 mm deep, with its side surfaces opened outwards. The edge of the "bowl" was thinned to about 1 mm. Occasionally, an almost regular ring of diameter about 14–15 mm was torn away from it.

In a single case, such a ring was observed to be pushed upon the electrode, i.e. "against" the plasma packet moving out of the generator (Fig. 3).

3.2. Coating material

3.2.1. Phase composition

Table II gives X-ray diffraction analysis results for the coating material made on a number of samples placed 200–270 mm from generator outlet along its axis (samples denoted "c") and 45 mm away from the axis (samples denoted "z").

The following phases were identified in the coating material:

0022–2461/91 $03.00 + .12

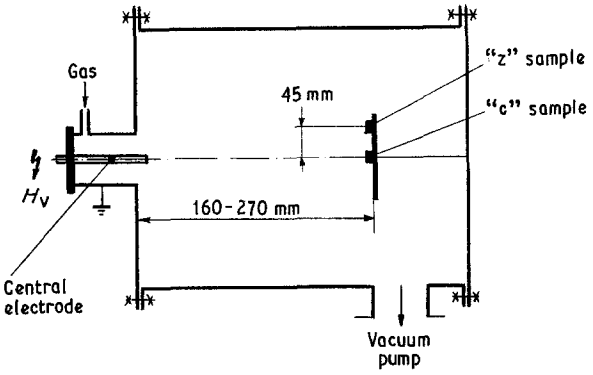

Figure 1 Schematic drawing of the apparatus.

TABLE I Phase composition of the central electrode material of the plasma generator

Experimental results		ASTM			
		(Co), 15-806		β-AlCo, 3-1192	
d (nm)	I/I_0	d (nm)	I/I_0	d (nm)	I/I_0
0.207	100	0.204	100		
0.179	30	0.177	40		
0.127	30	0.125	20	0.128	90
0.117	10			0.117	10

(i) a solid solution of alloy elements in cobalt (the matrix material of the internal electrode) and probably the β-AlCo phase (the other phase component of the material of the central electrode),

(ii) the Cr and CrCo phases which do not occur in the material of the central electrode.

A semi-quantitative analysis of the diffractograms obtained was also made, assuming that the absolute intensities of the respective "peaks" (to a first approximation) may be taken as indicators of the contents of the individual phases in the coating material crystallized on substrates positioned in various places of the crystallization chamber. The absolute heights of the "peaks" observed in the diffractograms were compared with the absolute heights of the peaks corresponding to 200c samples (Table III).

The results of the semi-quantitative analysis indicate that:

(a) the content of the solid solution Co(Cr, Al) in the coating material probably increases with increasing distance between the substrate and the plasma generator,

(b) the Cr and (CrCo) phases mostly occur in samples positioned axially; the contents of these phases in the coating material probably decrease as the distance between the substrates and the outlet of the plasma generator increases.

3.2.2. Chemical composition

Table IV gives the chemical compositions of the coatings deposited on substrates placed along the axis of the plasma generator, 250 mm away from its outlet. The surface areas examined were 24×10^4 μm^2.

From Table IV it can be seen that essentially the chemical composition of the coatings is similar to that of the starting material, i.e. the material of the central electrode of the plasma generator.

3.2.3. Morphology of the coating material

Fig. 4 shows the morphology of the surface (SEM) and a cross-section of the coating crystallized on a substrate placed at a distance of 160 mm from the outlet of the plasma generator. The voltage across the condenser battery was 7 kV and its capacitance was 175 μF. As can be seen, the coating is continuous and contains no cracks. Its porosity, determined by the metallographic method using an automatic TV picture analyser, was 1.9%, the average deviation being 0.178%. The high density seems to be associated with the submicroscopic size of the particles that build up the material of the coating. TEM observations showed that the size of the single particles was in order of

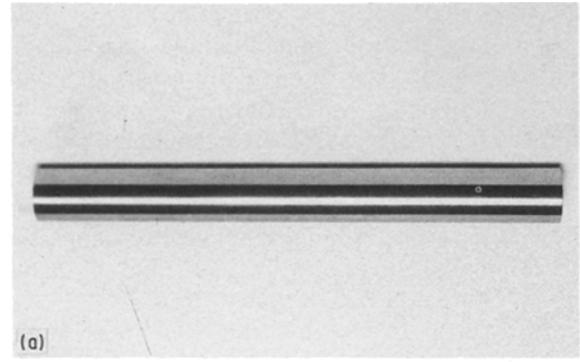

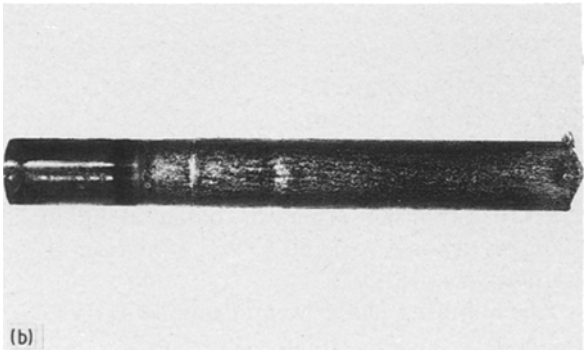

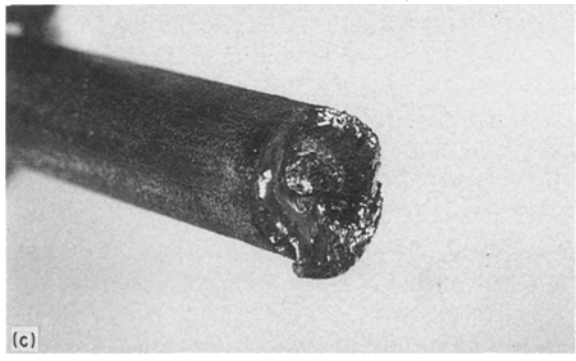

Figure 2 Internal electrode of the plasma generator (a) before the process, (b) after more than 15000 pulses, (c) free end of the electrode.

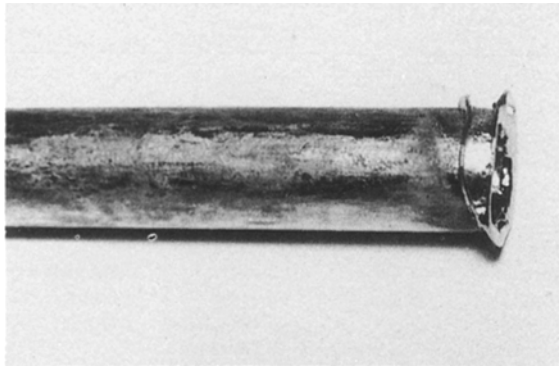

Figure 3 The edge of the free end of the electrode being torn away and shifted in a direction opposite to the plasma movement.

micrometres (Fig. 5). By using the Scherrer formula, the size of the particles of the solid solution was estimated to be 15 nm. The submicroscopic size of particles building up the coating obtained in the present investigations is in good agreement with the results obtained for diamond and TiN particles [6, 7].

It is interesting to compare the hardness of the coating material and that of their source material, i.e. the material of the inner electrode. The microhardness of the coating material, measured using the Vickers methods, was 1330 $H_{V_{20}}$, whereas the hardness of the material of the central electrode was 50 H_{RC} on the Rockwell scale which may be estimated to be equal to about 500–600 H_V.

3.3. Substrate material

The state of the substrates material was estimated using the same method as before, i.e. by comparing quantitatively the following values, read from the diffractograms: i.e. the relative heights of the peaks corresponding to the substrate material after the plasma process, were compared with the relative heights of the peaks characteristic of Ni (according to ASTM). The results of these comparisons are given in Table V.

4. Discussion

Based on the observations and results described above and taking into account the state of the matter we have formulated a hypothetical mechanism of crystallization of metallic CoCr Al coatings with the participation of pulsed plasma. The mechanism involves the following elementary steps:

(a) discharging of the condenser battery leads to shock ionization of gas in the generator;

TABLE II Phase compositions of the coating material deposited on substrate placed at various distances from the outlet of the plasma generator

(a) Experimental results

200c		250c		270c		200z		250z		270z		Identified phases
d (nm)	I/I_0	d (nm)	I/I_0	d (nm)	I/I_0	d (nm)	I/I_0	d (nm)	I/I_0	d (nm)	I/I_0	
0.2080	20	0.2080	19	0.2080	40	0.2075	23	0.2088	42	0.2075	38	Co(ss)
0.2043	10	0.2040	100	0.2037	88	0.2030	91	0.2037	100	0.2030	78	Ni
0.2014	72	0.2019	40	0.2017	11	0.2014	12	0.2019	27	–	–	CrCo
0.2000	42	0.2000	57	0.2000	12	0.2000	10	0.2000	25	–	–	CrCo
0.1800	7	0.1800	9	0.1800	32	0.1800	8	0.1790	10	0.1800	22	Co(ss)
0.1764	63	0.1763	74	0.1763	100	0.1766	100	0.1760	82	0.1768	100	Ni
0.1416	5	0.1412	5	–	–	0.1416	3	–	–	–	–	Cr
–	–	–	–	0.1274	6	0.1270	3	0.1275	8	0.1271	8	Co(ss) AlCo
0.1247	12	0.1249	26	0.1240	40	0.1244	18	0.1246	64	0.1245	63	Ni
0.1168	12	0.1167	7	–	–	–	–	–	–	–	–	Cr, CrCo, AlCo

(b) ASTM

Co, 15-806		Cr, 6-0694		CrCo, 9-52		β-AlCo, 3-1192		Ni, 4-850	
d (nm)	I/I_0	d (nm)	I/I_0	d (nm)	I/I_0	d (nm)	I/I_0	d (nm)	I/I_0
0.2047	100								
		0.2030	100						
				0.2014	50			0.2034	100
				0.1962	50				
				0.1926	100				
0.1772	40							0.1762	42
		0.1442	16						
0.1253	25								
				0.1257	50	0.128	90	0.1246	21
		0.1177	29						
				0.1175	50				
				0.1165	50	0.1177	100		

TABLE III Ratios of the absolute heights of the peaks corresponding to the coating material to the absolute heights of the peaks corresponding to the 200c sample

200c		200c	250c	270c	200z	250z	270z
d (nm)	I/I_0	I_{200c}/I_{200c}	I_{250c}/I_{200c}	I_{270c}/I_{200c}	I_{200z}/I_{200c}	I_{250z}/I_{200c}	I_{270z}/I_{200c}
0.208/Co	20	1.000	1.071	2.643	2.036	2.643	2.143
0.200/CrCo	72	1.000	0.928	0.223	0.277	0.357	deficiency
0.180/Co	7	1.000	1.111	8.444	2.222	2.222	4.444
0.141/Cr	5	1.000	0.900	deficiency	0.700	0.700	deficiency
0.127/CoAlCo	deficiency	deficiency	deficiency	present	present	present	present
0.117/CrCo AlCo	12	1.000	2.777	4.555	2.277	6.388	5.722

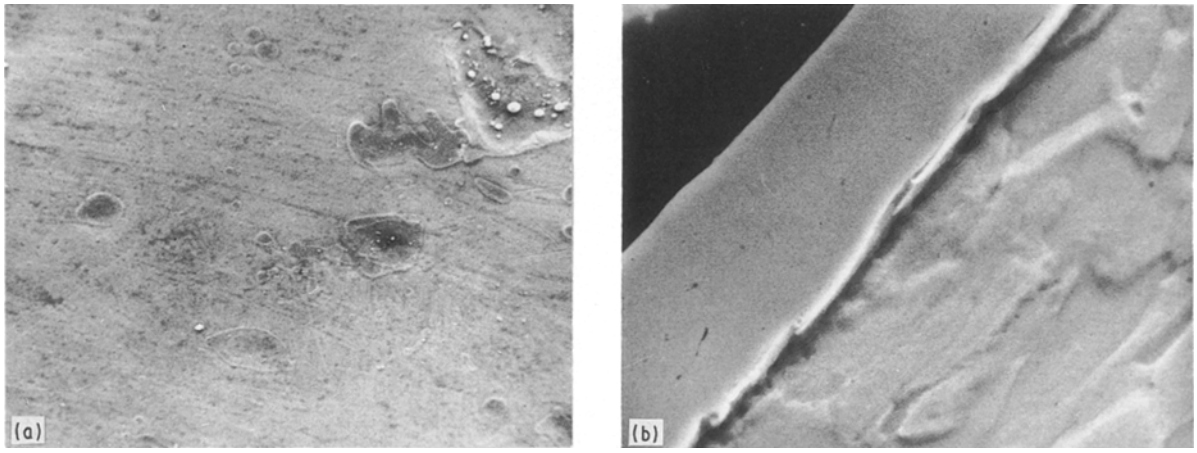

Figure 4 Scanning electron micrographs of (a) the surface and (b) cross-section of a sample crystallized on a substrate placed 160 mm apart from the generator; the voltage of the condenser battery was 6 kV, the capacitance of the condensers was 175 μF. (a) × 500; (b) × 2500.

TABLE IV Chemical composition of the material of the coatings (wt %)

Material	Element			
	Co	Cr	Al	Fe[a]
Central electrode	66	25	9	–
Coating	61.040	29.318	9.459	0.183

[a] Low-carbon steel was used in construction of the external generator electrode.

(b) the electrodynamic force [3]:

$$F = I^2 \ln a_2/a_1 \quad (1)$$

where I is the current in the electric circuit, a the diameter of the plasma accelerator electrode (2, external; 1, internal), exerted by the electromagnetic field accelerates the plasma, further ionization occurs;

(c) an electric arc of energy density $\sim 10^7\ \mathrm{J\,m^{-2}}$ (energy of one impulse ($\sim 10^3$ J)/surface of the plane of the free end of the central electrode ($\sim 10^{-4}\ \mathrm{m^2}$) over a very short time ($\sim 10^{-4}$ s) causes a portion of the electrode material to evaporate. An approximate calculation shows that the evaporation yield in one portion reaches $10\ \mathrm{g\,s^{-1}}$ (volume of portion $\sim 10^8\ \mu\mathrm{m}^3$, density of the material $\sim 10^{-11}\ \mathrm{g\,\mu m^{-3}}$, time $\sim 10^{-4}$ s). Under such conditions, the evaporation should proceed in an explosive manner, probably omitting the liquid phase, so that the segregation coefficients determining the proportions between the solid, the liquid and the gaseous phases of the individual components, and also their evaporation temperatures, have no significance here. This method of evaporation suggests that all the components of the electrode material contained in one portion evaporated simultaneously;

(d) the metal vapours are turned into a plasma state and are accelerated due to the electron–ion interaction within the plasma stream. Because the plasma particles move at a strongly directed, non-equilibrium velocity, it is only slightly probable that the plasmoid will be spread out by the diffusion;

(e) nucleation actually begins in the plasma, because of the rapid changes of supersaturation in time and space (as a consequence of the very short duration of the process). Nucleation is affected by the external electric field, as well as the electric charge of ions. As observed by Kashiev [11] and Rusanov [12], in the presence of electric field or ions, the critical nuclei are reduced in size;

(f) the thermodynamic conditions prevailing in regions where the plasmoid temperature is the highest, favour the formation of Cr clusters which are first to crystallize (because their crystallization temperature is the highest);

(g) the (CrCo) phase crystallizes heterogeneously on the Cr clusters thus formed. These two phases, i.e. Cr and (CrCo), predominate in those plasmoid regions

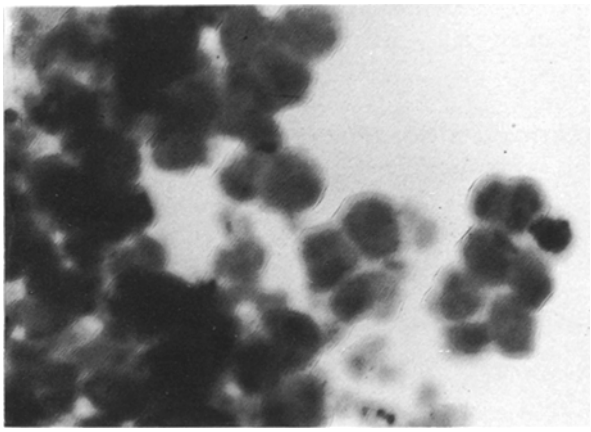

Figure 5 Transmission electron micrograph of particles building up the coating. × 200 000.

(especially the central region) where the thermodynamic temperature restricts the crystallization of the Co (Cr, Al) solid solution;

(h) the Co(Cr, Al) solid solution crystallizes heterogeneously on the existing clusters of the Cr and (CrCo) phases, as a result of which these two phases dissolve;

(i) the Co(Cr, Al) solid solution probably also crystallizes homogeneously in regions where the thermodynamic conditions (a lower thermodynamic temperature, strong oversaturation) favour this process;

(j) an ultrafine-grained coating, chiefly built up of the Co(Cr, Al) solution, is condensed on the substrate; the material of the coating is thermodynamically metastable in contrast to the two-phase material (solid solution + β-(CoAl) phase) of the inner electrode which is in a stable state;

(k) the plasmoid interacts in a pulse dynamic way with the substrate, heating the surface of the substrate during the pulses at a rate in order of 10^3 K/10^{-4} s. As a result, the substrates can be cleaned, which promotes adhesion. The surface region of the substrate (approximately 20 μm deep [13]) is probably heated to a more or less stationary temperature of about 700 K for a substrate positioned along the axis of the plasmoid (the recrystallization temperature of nickel is $T_R = 0.4\ T_L = 0.4 \times 1763$ K). In this sense the substrate surface is relatively cold during the plasma process (if the substrate temperature is of the order of 0.4 T_L the activation energy of processes that control the crystal growth on the substrate is a fraction of the activation energy needed for bulk diffusion [14]);

(l) during the plasma-generated temperature pulses, particles of the growing coating probably undergo a sort of sintering. The duration of the temperature pulses seems to be sufficient for the sintering but not sufficient to induce bulk diffusion.

The hypothetical mechanism described above permits us to explain the following experimental observations:

(i) the similarity between the chemical composition of the materials of the coating and of the inner electrode of the plasma generator;

(ii) the reduced contents of the Cr and (CrCo) phases with increasing distance (axial and radial) between the substrates and the generator outlet;

(iii) the fact that the density of the coating material is almost equal to the theoretical value;

(iv) the high hardness of the coating material;

(v) the probable recrystallization of the substrate material;

(vi) the shape of the internal electrode (especially the form of the free end of the electrode).

The absence of typical intergranular boundaries in the coating material requires separate consideration. It is difficult to describe the structure of the coating material using the three-zone model [15]. When considering coatings crystallized in pulsed plasma, it seems reasonable to supplement the three-zone model with an additional zone positioned between the zones I and II. This zone would represent the ultrafine-grained coating crystallized from pulsed plasma (whose thermodynamic temperature is of the order of 2000 K) on a relatively cold substrate subjected to cyclical heat pulses. The proposed region may be called the "freezing" zone.

It is worth commenting on the shape of the internal electrode after operation in an accelerator (Fig. 2b and c). The characteristic outwards opening of the free-end edge of the electrode, and mainly the observed pushing of the edge ring towards the accelerator, suggests that the plasma packet is moving out of the accelerator owing to a "counterdirectional" pressure. At the present stage of study it is difficult to identify the nature of this pressure, but it may appear as a result of the violent expansion of the plasma contained in the accelerator after the plasmoid "piston" has left it (cf. the "snow-plough" model proposed by Hart [3]).

4. Conclusions

A physico-chemical mechanism of crystallization of multi-component metallic coatings using the pulsed plasma method is described. The model for the process was based on the observations obtained by examining the characteristics of the coatings material obtained.

TABLE V Relative heights of the peaks of the substrate material after subjecting it to the plasma process, and the relative heights of the peaks characteristic of Ni (as given in ASTM). The relative heights of the peaks of the Ni sheet before plasma operation are given for comparison

Ni sheet		Ni, ASTM		200c	250c	270c	200z	250z	270z
d (nm)	I/I_0	d (nm)	I/I_0	I/I_0	I/I_0	I/I_0	I/I_0	I/I_0	I/I_0
0.2037	88	0.2034	100	100	100	99	92	100	86
0.1763	100	0.1762	42	55	71	100	100	87	100
0.1247	70	0.1246	21	15	35	57	18	78	93

According to the proposed model, the most essential features of this process are:

(i) the pulse character of the energy exchange processes;

(ii) the fact that the crystallization proceeds in the plasma and involves ions of evaporation products;

(iii) the non-equilibrium (anisotropic) distribution of the velocities of the plasma components.

Because of the pulse character of the energy exchange processes, the internal electrode material of the plasma generator evaporates in an explosive manner; the source of the vapour (the front face of the free end of this electrode) is well defined and constant in time and space. Owing to this evaporation mechanism and to the non-equilibrium distribution of the velocities of the particles within the plasma, the chemical composition of the coating material is a reproduction of that of the internal electrode.

The participation of an ion-induced electric field in the crystallization process carried out in plasma results in an ultrafine-crystalline structure of the alloy coating thus produced, the coating being chiefly built up of a supersaturated solid solution. This ultrafine-crystalline structure is obtained due to the "freezing" of the clusters formed on a relatively cold substrate whose surface is heated by plasma pulses. It is proposed that the ultrafine crystalline structure of the coating material should be represented in the three-zone model [15] as a fourth, "freezing" zone.

Finally, it should be noted that our observations of the chemical and phase compositions of the coating material, for example Fe (Co, Ni, Ti, Al, Cu) coatings [16], were similar. The proposed model thus seems to represent well the physical and chemical processes that proceed during pulsed plasma crystallization and may be considered to be applicable to the crystallization of any alloy metallic coating.

Acknowledgement

This work was supported by the State Office for Science and Technological Development under contract CPBR 2.4.

References

1. M. SOKOŁOWSKI, *J. Crystal Growth* **46** (1979) 136.
2. A. RUSEK and K. ZDUNEK, *Vacuum* **1** (1989) 55.
3. P. J. HART, *Phys. Fluids* **1** (1962) 38.
4. M. SOKOŁOWSKI, A. SOKOŁOWSKA, B. GOKIELI, A. MICHALSKI, A. RUSEK and Z. ROMANOWSKI, *J. Crystal Growth* **47** (1979) 421.
5. A. MICHALSKI and A. SOKOŁOWSKA, *J. Mater. Sci.* **20** (1985) 1842.
6. A. MICHALSKI and Z. ROMANOWSKI, *J. Crystal Growth* **61** (1983) 675.
7. A. SOKOŁOWSKA, K. ZDUNEK, H. GRIGORIEW and Z. ROMANOWSKI, *J. Mater. Sci.* **21** (1986) 763.
8. M. SOKOŁOWSKI, *J. Crystal Growth* **54** (1981) 519.
9. A. MICHALSKI and A. SOKOŁOWSKA, in "Proceedings VII ICCG", 1/80, Stuttgart 1983, 1.80.
10. K. ZDUNEK, in "Proceedings of the 4th Conference of CMES HTI", Nanjing 1987, p. 235.
11. D. KASHCHIEV, *J. Crystal Growth* **13/14** (1972) 128.
12. A. RUSANOV, *J. Colloid Interface Sci.* **1** (1979) 32.
13. A. MICHALSKI, *J. Mater. Sci. Lett.* **3** (1984) 505.
14. B. MOWCZAN and J. MALASZENKO, "Zarostoikie Pokrytia Osazdajemyje w Wakuumie" (Naukowa Dumka, Kijew, 1983).
15. B. MOWCZAN and A. DEMCZYSZYN, *Fiz. Met. Metall.* **28** (1969) 83.
16. K. ZDUNEK, to be published.

Received 19 April
and accepted 30 November 1990